

# Role Played by Surface Plasmons on Plasma Instability in Composite Layered Structures

Godfrey Gumbs<sup>1,2</sup>, Andrii Iurov<sup>1\*</sup> and Danhong Huang<sup>3</sup>

<sup>1</sup>*Department of Physics and Astronomy,*

*Hunter College of the City University of New York,*

*695 Park Avenue, New York, NY 10065, USA*

<sup>2</sup>*Donostia International Physics Center (DIPC),*

*P de Manuel Lardizabal, 4, 20018 San Sebastian, Basque Country, Spain*

<sup>3</sup>*Air Force Research Laboratory, Space Vehicles Directorate,*

*Kirtland Air Force Base, NM 87117, USA*

(Dated: October 13, 2014)

## Abstract

We demonstrate the engineering of a source of radiation from growing surface plasmons (charge density oscillations) in a composite nano-system. The considered hybrid nano-structure consists of a thick layer of a conducting substrate on whose surface a plasmon mode is activated conjoining a single or pair of thin sheets of either monolayer graphene, silicene or a two-dimensional electron gas as would occur at a hetero-interface. When an electric current is passed through either a layer or within the substrate, the low-frequency plasmons in the layer may bifurcate into separate streams due to the driving current. At a critical wave vector, determined by the separation between layers (if there are two) and their distance from the surface, their phase velocities may be in opposite directions and a surface plasmon instability leads to the emission of radiation (spiler). Spiler takes advantage of the flexibility of choosing its constituents to produce sources of radiation. The role of the substrate is to screen the Coulomb interaction between two layers or between a layer and the surface. The range of wave vectors where the instability is achieved may be adjusted by varying layer separation and type of material. Applications to detectors and other electromagnetic devices exploiting nano-plasmonics are discussed.

PACS numbers: 73.21.-b, 71.70.Ej, 73.20.Mf, 71.45.Gm, 71.10.Ca, 81.05.ue

---

\* E-mail contact: theorist.physics@gmail.com

## I. INTRODUCTION

Possible sources of terahertz (THz) radiation have been investigated for several years now. These frequencies cover the electromagnetic spectrum lying between microwave and infrared. By epitaxially growing layers of different semiconductors, high power THz quantum well layers emitting across a wide frequency range have been produced. The work reported so far covers ultra-long wavelength emission, phase/mode-locking, multiple color generation, photonic crystal structures, and improved laser performance with respect to both maximum operating temperature and peak output power. It was predicted by Kempa, et al.<sup>1</sup> (see also Ref. [2]) that when a current is passed through a stationary electron gas, the Doppler shift in response frequency of this two-component plasma leads to a spontaneous generation of plasmon excitations and subsequent Cherenkov radiation<sup>3</sup> at sufficiently high drift velocities. Similar conclusions are expected for monolayer graphene which is characterized by massless Dirac fermions where the energy dispersion is linear in the wave vector  $\mathbf{k}$  or a nanosheet of silicene consisting of silicon atoms, which has been synthesized<sup>4</sup>. In the same group of the periodic table with graphene, silicene is predicted to exhibit similar electronic properties. Additionally, it has the advantage over graphene in its compatibility with Si-based device technologies. The electrons in graphene with classical mobility estimated from  $\rho_{xx} = 1/ne\mu_c$  (with  $n$  as electron density) to be  $\mu_c \sim \times 10^5 \text{ cm}^2/V \cdot s$  may move ballistically over distances up to  $0.2 \mu m$ .

Plasmon modes of quantum-well transistor structures with frequencies in the THz range may be excited with the use of far-infrared (FIR) radiation. A split grating-gate design has been found to significantly enhance FIR response<sup>5-8</sup>. Additionally, the role played by plasma excitations in the THz response of low-dimensional microstructures has received considerable attention<sup>9-18</sup>. This paper discusses plasma instabilities in a pair of Coulomb coupled layers when the layers are either graphene, a two-dimensional electron gas (2DEG) or some other type of 2D-material layer in which inter-layer hopping between layers is not included.<sup>17,18</sup>

We consider a composite nano-system consisting of a thick layer of conducting substrate on whose surface the plasmon is activated in proximity with a pair of thin sheets. We demonstrate how the screening of the Coulomb coupling of the plasmons in this pair of layers by the charge density fluctuations on the surface of a semi-infinite substrate affects the surface plasmon instability that leads to the emission of radiation (spiler). The excitation

of these plasmon modes is induced by resonant external optical fields. As an emitter, the spiler may be activated optically. Spiler exploits the flexibility of choosing its constituents to produce coherent sources of radiation. Applications to sensors that electromagnetic devices exploiting nano-plasmonics are explored.

Our approach models an ensemble consisting of a pair of 2D layers and a thick layer of a conducting medium that emits radiation when an electric field splits the plasmon spectrum which results in an instability when the phase velocities associated with these plasmon branches have opposing signs at a common frequency.

## II. GENERAL FORMULATION OF THE PROBLEM

In our formalism, we consider a nano-scale system consisting of a pair of 2D layers and a thick conducting material. The layer may be monolayer graphene or a 2DEG such as a semiconductor inversion layer or HEMT (high electron mobility transistor). The graphene layer may have a gap, thereby extending the flexibility of the composite system that also incorporates a thick layer of conducting material as depicted in Fig. 1. The excitation spectra of allowable modes will be determined from a knowledge of the non-local dielectric function  $\epsilon(\mathbf{r}, \mathbf{r}'; \omega)$  which depends on position coordinates  $\mathbf{r}, \mathbf{r}'$  and frequency  $\omega$  or its inverse  $K(\mathbf{r}, \mathbf{r}'; \omega)$  satisfying  $\int d\mathbf{r}' K(\mathbf{r}, \mathbf{r}'; \omega) \epsilon(\mathbf{r}', \mathbf{r}''; \omega) = \delta(\mathbf{r} - \mathbf{r}'')$ . The self-consistent field equation for  $K(\mathbf{r}, \mathbf{r}'; \omega)$  is now determined.

In operator notation, the dielectric function for the 2D layer and semi-infinite structure is given by

$$\hat{\epsilon} = \hat{1} + \hat{\alpha}_{SI} + \hat{\alpha}_{2D} \equiv \hat{\epsilon}_{SI} + \hat{\alpha}_{2D} = \hat{K}_{SI}^{-1} + \hat{\alpha}_{2D} , \quad (1)$$

where  $\hat{\epsilon} = \hat{K}^{-1}$  with  $\hat{K}$  as the inverse dielectric function satisfying

$$\hat{K} = \hat{K}_{SI} - \hat{K}_{SI} \cdot \hat{\alpha}_{2D} \cdot \hat{K} . \quad (2)$$

Here,  $\hat{\alpha}$ ,  $\hat{\alpha}_{2D}$  and  $\hat{\alpha}_{SI}$  are the polarization functions of the composite system, the polarization function of the 2D layer and semi-infinite substrate, respectively. Additionally,  $\hat{K}_{SI}$  is the inverse dielectric function for the semi-infinite substrate whose surface lies in the  $z = 0$  plane. In integral form, after Fourier transforming with respect to coordinates parallel to

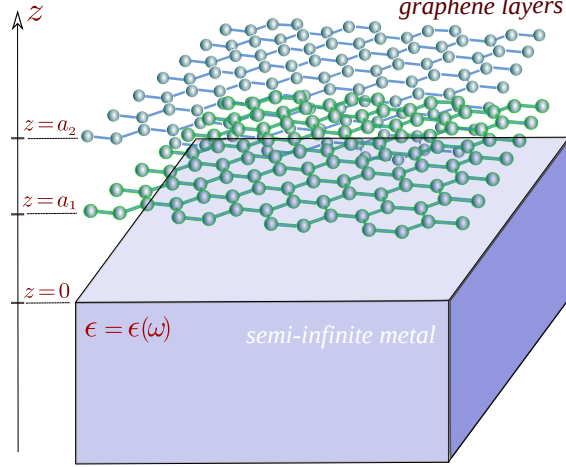


FIG. 1: (Color online) Schematic illustration of a spiler generator consisting of a thick (semi-infinite) conducting material on whose surface a plasmon resonance may induce an instability by coupling to the 2D plasmons on a pair of thin layers such as graphene, silicene or 2DEG at a hetero-interface.

the  $xy$ -plane and suppressing the in-plane wave number  $q_{\parallel}$  and frequency  $\omega$ , we obtain

$$K(z_1, z_2) = K_{SI}(z_1, z_2) - \int_{-\infty}^{\infty} dz' \int_{-\infty}^{\infty} dz'' K(z_1, z') \alpha_{2D}(z', z'') K(z'', z_2). \quad (3)$$

Here, the polarization function for the 2D structure is given by

$$\alpha_{2D}(z', z'') = \int_{-\infty}^{\infty} dz''' v(z' - z''') D(z''', z''), \quad (4)$$

where  $v(z - z') = (2\pi e^2 / \epsilon_s q_{\parallel}) \exp(-q_{\parallel} |z - z'|)$ ,  $\epsilon_s = 4\pi\epsilon_0\epsilon_r$ , and the 2D response function obeys

$$D(z''', z'') = \Pi_{2D}^{(0)}(q_{\parallel}, \omega) \delta(z''' - a) \delta(z'' - a) \quad (5)$$

with  $\Pi_{2D}^{(0)}(q_{\parallel}, \omega)$  as the single-particle in-plane response. Upon substituting this form of the polarization function for the monolayer into the integral equation for the inverse dielectric function, we have

$$K(z_1, z_2) = K_{SI}(z_1, z_2) - \Pi_{2D}^{(0)}(q_{\parallel}, \omega) \int_{-\infty}^{\infty} dz' K_{SI}(z_1, z') v(z' - a) K(a, z_2). \quad (6)$$

We now set  $z_1 = a$  in Eq. (6) and obtain

$$K(a, z_2) = K_{SI}(a, z_2) - \Pi_{2D}^{(0)}(q_{||}, \omega) \left\{ \int_{-\infty}^{\infty} dz' K_{SI}(a, z') v(z' - a) \right\} K(a, z_2) . \quad (7)$$

Solving for  $K(a, z_2)$  yields

$$K(a, z_2) = \frac{K_{SI}(a, z_2)}{S_C(q_{||}, \omega)} , \quad (8)$$

and

$$S_C(q_{||}, \omega) \equiv 1 + \Pi_{2D}^{(0)}(q_{||}, \omega) \left\{ \int_{-\infty}^{\infty} dz' K_{SI}(a, z') v(z' - a) \right\} \quad (9)$$

whose zeros determine the plasmon resonances. In our numerical calculations, we shall use  $K_{SI}(z, z')$  given in Eq. (30) of Ref. [19]. Thus, from Eq. (6), we obtain

$$K(z_1, z_2) = K_{SI}(z_1, z_2) - \Pi_{2D}^{(0)}(q_{||}, \omega) \frac{K_{SI}(a, z_2)}{S_C(q_{||}, \omega)} \left\{ \int_{-\infty}^{\infty} dz' K_{SI}(z_1, z') v(z' - a) \right\} . \quad (10)$$

In the local limit, we have

$$S_C(q_{||}, \omega) = 1 + \frac{2\pi e^2}{\epsilon_s q_{||}} \Pi_{2D}^{(0)}(q_{||}, \omega) \left\{ 1 + e^{-2q_{||}a} \frac{1 - \epsilon_B(\omega)}{1 + \epsilon_B(\omega)} \right\} . \quad (11)$$

With  $\Pi_{2D}^{(0)}(q_{||}, \omega) \approx C q_{||}^2 / \omega^2$ , we obtain the following equation:

$$1 - \frac{2\pi C e^2}{\epsilon_s \omega^2} q_{||} \left\{ 1 + e^{-2q_{||}a} \frac{\omega_p^2}{2\omega^2 - \omega_p^2} \right\} = 0 , \quad (12)$$

which is a quadratic equation for  $\omega^2$ . For a 2DEG, we have  $C = n_{2D}/m_{2D}^*$ . For graphene,

$$C = \frac{2\mu}{\pi \hbar^2} \left\{ 1 - \frac{\Delta^2}{\mu^2} \right\} , \quad (13)$$

where  $\mu$  is the chemical potential and  $\Delta$  is the gap between valence and conduction bands. Consequently, we find the plasmon frequency as follows:<sup>20</sup>

$$\omega^2 = K_1 \pm \sqrt{K_2} \quad (14)$$

with  $K_1$  and  $K_2$  defined by:

$$\begin{aligned}
K_1 &= \frac{\pi e^2 C}{\epsilon_s} q_{\parallel} + \left( \frac{\omega_p}{2} \right)^2 , \\
K_2 &= \frac{\pi e^2 C \omega_p^2}{\epsilon_s} e^{-2q_{\parallel} a} q_{\parallel} + \left[ \left( \frac{\omega_p}{2} \right)^2 - \frac{C e^2 \pi}{\epsilon_s} q_{\parallel} \right]^2 .
\end{aligned} \tag{15}$$

In the long-wavelength limit ( $q_{\parallel} \ll k_F$ ) these expressions are reduced to:

$$\begin{aligned}
\omega_1^2 &\approx \frac{4\pi C e^2 a}{\epsilon_s} q_{\parallel}^2 , \\
\omega_2^2 &\approx \frac{\omega_p^2}{2} + \frac{2\pi C e^2}{\epsilon_s} q_{\parallel} ,
\end{aligned} \tag{16}$$

and the frequencies are

$$\begin{aligned}
\omega_1 &\approx 2e \sqrt{\frac{\pi a C}{\epsilon_s}} q_{\parallel} , \\
\omega_2 &\approx \frac{\omega_p}{\sqrt{2}} + \frac{\sqrt{2}\pi C e^2}{\epsilon_s \omega_p} q_{\parallel} ,
\end{aligned} \tag{17}$$

which are both linear in  $q_{\parallel}$ , unlike the  $q_{\parallel}^{1/2}$ -dependence for free-standing graphene or the 2DEG<sup>12–15,21,22</sup>.

We may generalize the formalism to a structure with a double layer positioned at  $z = a_1$  and  $z = a_2$  ( $0 < a_1 < a_2$ ) interacting with each other as well as the semi-infinite conducting substrate with its surface located at  $z = 0$ . A similar calculation shows that

$$\begin{aligned}
K(z_1, z_2) &= K_{SI}(z_1, z_2) - \Pi_{2D;1}^{(0)}(q_{\parallel}, \omega) \int_{-\infty}^{\infty} dz' K_{SI}(z_1, z') v(z' - a_1) K(a_1, z_2) \\
&- \Pi_{2D;2}^{(0)}(q_{\parallel}, \omega) \int_{-\infty}^{\infty} dz' K_{SI}(z_1, z') v(z' - a_2) K(a_2, z_2) .
\end{aligned} \tag{18}$$

By setting  $z_1 = a_1$  and  $z_1 = a_2$  in turn in Eq.(18) and solving the pair of simultaneous equations for  $K(a_1, z_2)$  and  $K(a_2, z_2)$ , we obtain

$$\begin{bmatrix} K(a_1, z_2) \\ K(a_2, z_2) \end{bmatrix} = \frac{1}{S_c^{(2)}(q_{\parallel}, \omega)} \vec{\mathcal{M}}(q_{\parallel}, \omega) \begin{bmatrix} K_{SI}(a_1, z_2) \\ K_{SI}(a_2, z_2) \end{bmatrix} , \tag{19}$$

where  $S_c^{(2)}(q_{\parallel}, \omega) = \text{Det} \vec{\mathcal{M}}(q_{\parallel}, \omega)$  with

$$\begin{aligned} \vec{\mathcal{M}}(q_{\parallel}, \omega) = & \\ \begin{bmatrix} 1 + \Pi_{2D;2}^{(0)}(q_{\parallel}, \omega) \int_{-\infty}^{\infty} dz' K_{SI}(a_2, z') v(z' - a_2) & -\Pi_{2D;2}^{(0)}(q_{\parallel}, \omega) \int_{-\infty}^{\infty} dz' K_{SI}(a_1, z') v(z' - a_2) \\ -\Pi_{2D;1}^{(0)}(q_{\parallel}, \omega) \int_{-\infty}^{\infty} dz' K_{SI}(a_2, z') v(z' - a_1) & 1 + \Pi_{2D;1}^{(0)}(q_{\parallel}, \omega) \int_{-\infty}^{\infty} dz' K_{SI}(a_1, z') v(z' - a_1) \end{bmatrix}. \end{aligned} \quad (20)$$

Substituting the results for  $K(a_1, z_2)$  and  $K(a_2, z_2)$  into Eq. (18), we obtain the complete inverse dielectric function for a pair of 2D planes interacting with each other and a semi-infinite conducting material. The plasmon excitation frequencies are determined by the zeros of  $S_c^{(2)}(q_{\parallel}, \omega)$ . Furthermore, the effect of the inverse dielectric function for the semi-infinite structure  $K_{SI}(z, z'; q_{\parallel}, \omega)$  screens coupling within and between two layers. As a matter of fact, our result for the plasmon dispersion relation generalizes that obtained by Das Sarma and Madhukar<sup>23</sup> for a bi-plane. In the current case, we obtain in the local limit

$$\begin{aligned} S_c^{(2)}(q_{\parallel}, \omega) = & \left\{ 1 + \frac{2\pi e^2}{\epsilon_s q_{\parallel}} \Pi_{2D;2}^{(0)}(q_{\parallel}, \omega) \left[ 1 + e^{-2q_{\parallel} a_2} \frac{\omega_p^2}{2\omega^2 - \omega_p^2} \right] \right\} \\ & \times \left\{ 1 + \frac{2\pi e^2}{\epsilon_s q_{\parallel}} \Pi_{2D;1}^{(0)}(q_{\parallel}, \omega) \left[ 1 + e^{-2q_{\parallel} a_1} \frac{\omega_p^2}{2\omega^2 - \omega_p^2} \right] \right\} \\ & - \left( \frac{2\pi e^2}{\epsilon_s q_{\parallel}} \right)^2 \Pi_{2D;1}^{(0)}(q_{\parallel}, \omega) \Pi_{2D;2}^{(0)}(q_{\parallel}, \omega) \left[ e^{-q_{\parallel}|a_1 - a_2|} + e^{-q_{\parallel}(a_1 + a_2)} \frac{\omega_p^2}{2\omega^2 - \omega_p^2} \right]^2. \end{aligned} \quad (21)$$

We now introduce our notation,  $\bar{C}_j = 2\pi e^2 C_j / (\epsilon_s \omega_p^2)$  for  $j = 1, 2$ . The spectral function yields real frequencies. A plane interacting with the half-space has two resonant modes. Each pair of 2D layers interacting in isolation far from the half-space conducting medium supports a symmetric and an antisymmetric mode<sup>23</sup>. In the absence of a driving current, the analytic solutions for the plasmon modes for a pair of 2D layers that are Coulomb coupled to a half-space are given by

$$\begin{aligned} \Omega_1(q_{\parallel})/\omega_p &= 1/\sqrt{2} + q_{\parallel} (\bar{C}_1 + \bar{C}_2)/\sqrt{2} + \mathcal{O}[q_{\parallel}^2], \\ \Omega_2(q_{\parallel})/\omega_p &= q_{\parallel} \sqrt{\bar{C}_1 a_1 + \bar{C}_2 a_2 + \sqrt{\mathcal{A}}} + \mathcal{O}[q_{\parallel}^2], \\ \Omega_3(q_{\parallel})/\omega_p &= q_{\parallel} \sqrt{\bar{C}_1 a_1 + \bar{C}_2 a_2 - \sqrt{\mathcal{A}}} + \mathcal{O}[q_{\parallel}^2], \end{aligned} \quad (22)$$

where  $\mathcal{A} \equiv (\overline{C}_1 a_1 - \overline{C}_2 a_2)^2 + 4\overline{C}_1 \overline{C}_2 a_1^2$  and the term  $4\overline{C}_1 \overline{C}_2 a_1^2$  plays the role of “Rabi coupling”. Clearly, for long wavelengths, only  $\Omega_1(q_{\parallel})$  depends on  $\omega_p$ . However, the excitation spectrum changes dramatically when a current is driven through the configuration. Under a constant electric field, the carrier distribution is modified, as may be obtained by employing the relaxation time approximation in the equation of motion for the center-of-mass momentum. For carriers in a parabolic energy band with effective mass  $m^*$  and drift velocity  $\mathbf{v}_d$  determined by the electron mobility and the external electric field, the electrons in the medium are redistributed. This is determined by a momentum shift in the wave vector  $\mathbf{k}_{\parallel} \rightarrow \mathbf{k}_{\parallel} - m^* \mathbf{v}_d / \hbar$  in the thermal-equilibrium energy distribution function  $f_0(\epsilon_{\mathbf{k}})$ . By making a change of variables in the well-known Lindhard polarization function  $\Pi_{2D}^{(0)}(q_{\parallel}, \omega)$ , this effect is equivalent to a frequency shift  $\omega \rightarrow \omega - \mathbf{q}_{\parallel} \cdot \mathbf{v}_d$ . For massless Dirac fermions in graphene with linear energy dispersion, this Doppler shift in frequency is not in general valid for arbitrary wave vector as we prove in our Appendix. This is our conclusion after we relate the surface current density to the center-of-mass wave vector in a steady state. Our calculation shows that the redistribution of electrons leads to a shift in the wave vector appearing in the Fermi function by the center-of-mass wave vector  $\mathbf{K}_0 = (k_F/v_F)\mathbf{v}_d$  where  $k_F$  and  $v_F$  are the Fermi wave vector and velocity, respectively. However, in the long wavelength limit,  $q_{\parallel} \rightarrow 0$ , the Doppler shift in frequency is approximately obeyed. This is discussed in Appendix A. Consequently, regardless of the nature of the 2D layer represented in the dispersion equation we may replace  $\omega \rightarrow \omega - \mathbf{q}_{\parallel} \cdot \mathbf{v}_d$  in the dispersion equation in the presence of an applied electric field at long wavelengths.

We shall treat the solution frequencies  $\omega_{\pm}(q_{\parallel})$  as complex variables with  $\text{Im}[\omega_{\pm}(q_{\parallel})] \geq 0$ , where  $\text{Im}[\omega_{\pm}(q_{\parallel})] > 0$  implies a finite growth rates  $\gamma_{\pm}(q_{\parallel}) = \text{Im}[\omega_{\pm}(q_{\parallel})]$  for two split plasmon modes. Since  $\epsilon(q_{\parallel}, \omega)$  is a complex function, we ask for  $\text{Re}[\epsilon(q_{\parallel}, \omega)] = \text{Im}[\epsilon(q_{\parallel}, \omega)] = 0$ . Therefore, we are left with damping-free plasmon modes in the system but they still face possible instability due to  $\text{Im}[\omega_{\pm}(q_{\parallel})] > 0$ .

### III. NUMERICAL RESULTS AND DISCUSSION

First, we have investigated numerically the effect of passing a current through a layer of 2DEG, graphene or silicene in the presence of a surface, for a pair of 2D layers and a semi-infinite conducting medium as presented in Fig. 1. In Fig. 2, we present the complex



frequencies which yield the plasmon dispersion (real part) and inverse lifetime (imaginary part). The layers are located at  $z = a_1 = 0.1 \bar{C}_1$  and  $z = a_2 = 0.4 \bar{C}_1$ . Each panel presents results for a different drift velocity  $v_d/\omega_p = 0, 0.5 \bar{C}_1, 0.8 \bar{C}_1$  and  $1.6 \bar{C}_1$ . In the absence of a drift current, ( $v_d = 0$ ), panel (a) shows that there are three plasmon branches excited, which are stable as given by Eq. (23). At low drift velocity, panel (b) shows that the plasmons are still stable. However, as the current is increased, the lowest branches may become unstable as demonstrated in panels (c) and (d) through the appearance of a finite imaginary part for the frequency. The carrier concentrations, chemical potentials or temperatures in the layers are such that  $\bar{C}_1 = 1.2 \bar{C}_2$  for all cases. Either of the two lowest plasmon branches might become unstable, depending on the strength of the drift current. The Rabi splitting of the plasmon branches in the presence of an external electric field is a consequence of quasiparticles having different energies for the same wavelength.

From the perspective of real space, the plasmon wave is a longitudinal charge density wave with both its density fluctuation and phase velocity  $v_p$  along the  $\mathbf{q}_{\parallel}$  (propagation) direction. When there are two electron gas layers separated by a distance  $\Delta a$  in the  $z$  direction, the inter-layer coulomb coupling will produce two plasmon modes with different energy dispersions  $\omega_{\pm}(q_{\parallel})$  and phase velocities  $v_{\pm}(q_{\parallel}) = \omega_{\pm}(q_{\parallel})/q_{\parallel}$ , which are separately associated with the symmetric [in-phase, upper  $\omega_{+}(q_{\parallel})$  branch in Fig. 2(a)] and antisymmetric [out-of-phase, lower  $\omega_{-}(q_{\parallel})$  branch] states of charge-density waves. The symmetric plasmon mode gives rise to a dipole-like plasmon excitation, similar in nature to that of a single layer with an electron density given by adding the densities on the two layers. On the other hand, the antisymmetric plasmon mode leads to a quadruple-like excitation, which is able to store electric field energy between the two layers. In the presence of a current with drift velocity  $v_d$  for electrons in one of the two electron-gas layers, the phase velocities of these two spatially separated plasmon modes are modified drastically due to the Doppler shift as well as the surface plasmon on the substrate. Consequently, two streams of quasiparticles with different phase velocities may be created from either the symmetric or antisymmetric mode, depending on the strength of the current, the separation between layers and their distances from the surface of the substrate. However, for freely suspended layers, the lower-energy antisymmetric plasmon mode becomes unstable whenever  $v_d$  lies within the range  $v_{-}(q_{\parallel}) < v_d < v_{+}(q_{\parallel})$ , switching from a quadruple-like excitation to a dipole-like excitation. The instability for the plasmon mode has a finite lifetime because it grows after taking

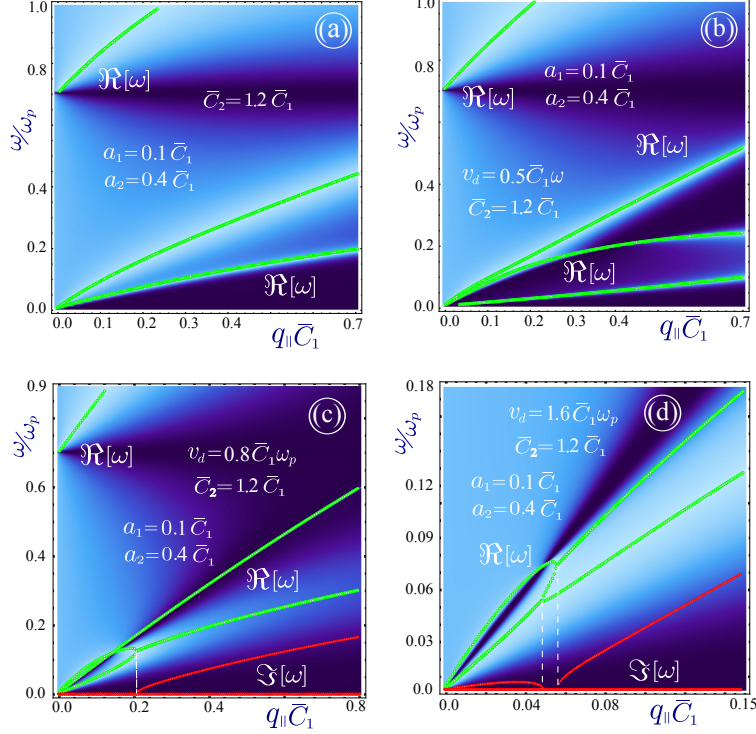


FIG. 2: (Color online) Complex frequencies  $\omega$  yielding the plasmon dispersion (real part  $\Re[\omega]$ ) and inverse lifetime (imaginary part  $\Im[\omega]$ ) for a pair of 2D layers and a semi-infinite conducting medium as presented in Fig. 1. The plasma frequency for the semi-infinite medium is  $\omega_p$ . The layers are located at  $a_1 = 0.1 \bar{C}_1$  and  $a_2 = 0.4 \bar{C}_1$  with respect to the surface. Each panel corresponds to a different drift velocity  $v_d/\omega_p = 0, 0.5 \bar{C}_1, 0.8 \bar{C}_1$  and  $1.6 \bar{C}_1$ . Panel (a) with  $v_d = 0$  corresponds to the solutions in Eq. (23). Panel (b) shows that for a small drift  $v_d$  additional plasmon branch appears, but all solutions are stable. The carrier concentrations, chemical potentials or temperatures in the layers are such that  $\bar{C}_1 = 1.2 \bar{C}_2$  for all cases. Either of the two lowest plasmon branches might become unstable, depending on  $v_d$ . The Rabi splitting of the plasmon excitation branches by the external electric field is attributed to quasiparticles with different excitation energies for the same wavelength. After the “loop” closes in (c), the lowest branch becomes unstable with finite imaginary part illustrated by the red curve. In (d), the lowest plasmon branch has an instability for two separate ranges of wave vector.

energy from the injected current and transferring it to the incident electromagnetic field.

From the point of view of momentum space, electrons may only occupy momentum space within the range of  $|\mathbf{k}_{||}| \leq k_F$  at zero temperature in a state of thermal equilibrium, where

$k_F$  is the electron Fermi wave number and  $\varepsilon(k_F) = \varepsilon(-k_F) = E_F$  is the Fermi energy. When a current is passed through the electron gas, electrons are driven out from this state of thermal equilibrium and their population becomes asymmetrical with respect to  $k_{\parallel} = 0$ . In this case, the Fermi energy  $E_F$  is split into  $E_{F,+} = \varepsilon(k_F + K_c)$  and  $E_{F,-} = \varepsilon(-k_F + K_c)$  with  $E_{F,+} > E_{F,-}$ , where  $\hbar K_c$  represents the electron center-of-mass momentum. In this shifted Fermi-Dirac distribution model, electrons in such a non-equilibrium state are energetically unstable, and the higher-energy electrons in the range  $k_F \leq k_{\parallel} \leq k_F + K_c$  tend to relax to the lower-energy empty states in the range of  $-k_F \leq k_{\parallel} \leq K_c - k_F$  by emitting electromagnetic waves and phonons to ensure total momentum and energy conservation. This process is known as radiation loss of plasmon excitations in the time domain, in addition to the usual absorption loss of plasmon excitations in the space domain due to nonzero imaginary part of the electron dielectric function.

A surface grating must be employed in order to convert the energy of the unstable plasmon mode into a transverse radiation field in free space and at the same time suppress phonon emission (heating). The growth rate  $\gamma_p(q_{\parallel}) = \text{Im}[\omega_p(q_{\parallel})]$  of the plasmon mode is determined by the imaginary part of the plasmon frequency while the average plasmon growth rate (per unit area) is given by  $\gamma(K_c) = (2\pi)^{-1} \int_0^{\infty} dq_{\parallel} \gamma_p(q_{\parallel}) q_{\parallel}$ .

#### IV. CONCLUDING REMARKS

In summary, we are proposing a spiler quantum plasmonic device which employs 2D layers in combination with a thick conducting material. We find that the spiler emits electromagnetic radiation when a current is passed through the 2D layer or the surface of the thick conducting material to make the plasmons become unstable at a specific frequency and wave number. It is possible to change the range of plasmon instability by selecting the properties of the nanosheet or frequency of the surface plasmon, i.e., the substrate. The surface plasmon plays a crucial role in giving rise to the Rabi splitting and the concomitant streams of quasiparticles whose phase velocities are in opposite directions when the instability takes place. The emitted electromagnetic radiation may be collected from regions on the surface that are convenient. Finally, we note that in presenting our numerical results, we measured frequency in terms of the bulk plasmon frequency which, typically for heavily-doped semiconductors, we have  $\hbar\omega_p \sim 0.5 \text{ eV}$ . Either for intrinsic graphene, doped monolayer graphene

or an inversion layer 2DEG, we have  $\overline{C} \sim 10^{-4} \text{ m}$  and  $v_d \sim 10^6 \text{ m/s}$ . In Fig. 2, the unit of frequency is  $\omega_0 = \sqrt{2\pi e^2 C_1 k_F / \epsilon_s}$  which is of the same order as  $\omega_p$ .

The current-driven asymmetric electron distribution in  $k$  space leads to an induced polarization current or a “dipole radiator”. If two electron gas layers are placed close enough, the in-phase inter-layer Coulomb interaction will give a dipole-like plasmon excitation, similar to that of a single layer. On the other hand, the out-of-phase layer Coulomb coupling will lead to an unstable quadruple-like excitation. This unstable quadruple-like plasmon excitation can be effectively converted into a transverse electromagnetic field in free space if a surface grating is employed.

### Acknowledgments

This research was supported by contract # FA 9453-13-1-0291 of AFRL. DH would like to thank the Air Force Office of Scientific Research (AFOSR) for its support. We acknowledge having helpful discussions with Oleksiy Roslyak and Antonios Balassis.

### Appendix A: Effect of Drift Current on the Polarization

Let us first consider the case when a current is passed through a 2DEG layer. This current creates a Doppler shift in the response function  $\Pi(q, \omega - \mathbf{q} \cdot \mathbf{v}_d)$ . The derivation is presented in the paper by Kempa, et al.<sup>1</sup> and the argument is as follows. The energy dispersion for an electron in a 2DEG is  $\epsilon_{\mathbf{k}} = \hbar^2 \mathbf{k}^2 / 2m^*$ , where  $m^*$  is the electron effective mass. The current flow leads to the replacement in wave vector  $\mathbf{k} \rightarrow \mathbf{k} - m^* \mathbf{v}_d / \hbar$  everywhere in the polarization function

$$\Pi(\mathbf{q}, \omega) = 2 \int \frac{d^2 \mathbf{k}}{(2\pi)^2} \frac{f_0(\epsilon_{|\mathbf{k}-\mathbf{q}|}, T) - f_0(\epsilon_{\mathbf{k}}, T)}{\epsilon_{|\mathbf{k}|} - \epsilon_{|\mathbf{k}-\mathbf{q}|} - \hbar(\omega + i0^+)} , \quad (\text{A1})$$

where  $f_0(\epsilon)$  is the equilibrium distribution function for electrons. After this wave vector replacement is carried out and a change of variables is made in the resulting integral, we simply obtain an expression for the polarization function which is exactly the same as that given in Eq. (A1), except with the frequency shifted by  $\mathbf{q} \cdot \mathbf{v}_d$ .

We now turn to the case of graphene which is characterized by massless Dirac fermions for

which the energy dispersion is linear in the wave vector  $\mathbf{k}$ . For a spatially-uniform system, the first-order moment of the Boltzmann equation for a single valley gives us

$$\frac{\partial \mathbf{j}(t)}{\partial t} = -\frac{\mathbf{j}(t)}{\tau_0} - N_c \frac{\nu_0^2 e}{2} \mathbf{F}(t) (k_B T) \mathcal{Q}_0(\eta) , \quad (\text{A2})$$

where  $N_c = 1/(\pi \hbar^2 \nu_0^2)$ ,  $\eta = \mu_0(t)/k_B T$ ,  $\mu_0$  is the chemical potential of electrons in graphene, the quantity

$$\mathcal{Q}_0(\eta) = \int_0^\infty \frac{dx}{e^{(x-\eta)} + 1} , \quad (\text{A3})$$

and

$$\mathbf{j}(t) = \frac{2}{\mathcal{A}} \sum_{\mathbf{k}} \mathbf{v}_k f_0(\varepsilon_k, T, t) , \quad (\text{A4})$$

is the electron surface current density,  $\mathcal{A}$  is the sample area,  $T$  is the electron temperature,  $\hbar \mathbf{k}$  is the electron wave vector,  $\varepsilon_k = \hbar \nu_0 k$  is the electron kinetic energy,  $\nu_0$  is the Fermi velocity of graphene,  $\mathbf{v}_k = \nabla_k \varepsilon_k / \hbar$  is the electron group velocity, and  $\tau_0$  is the average momentum-relaxation time,  $\mathbf{F}(t)$  is the external electric field. Additionally, we have the following relation

$$-N_c (k_B T) \mathcal{Q}_0(\eta) = \frac{2}{\mathcal{A}} \sum_{\mathbf{k}} \frac{\partial f_0(\varepsilon_k, T, t)}{\partial \varepsilon_k} , \quad (\text{A5})$$

$$\rho(t) = \frac{2}{\mathcal{A}} \sum_{\mathbf{k}} f_0(\varepsilon_k, T, t) , \quad (\text{A6})$$

where  $\rho(t)$  is the electron areal density. Considering a steady state under a constant electric field  $\mathbf{F}_0$ , we obtain

$$\mathbf{j}_0 = \frac{\hbar \nu_0^2}{2} \frac{e \tau_0}{\hbar} \mathbf{F}_0 \frac{2}{\mathcal{A}} \sum_{\mathbf{k}} \frac{\partial f_0(\varepsilon_k, T)}{\partial \varepsilon_k} . \quad (\text{A7})$$

At  $T \approx 0$  K, we have

$$\frac{2}{\mathcal{A}} \sum_{\mathbf{k}} \frac{\partial f_0(\varepsilon_k, T)}{\partial \varepsilon_k} \approx -\frac{E_F}{\pi \hbar^2 \nu_0^2} , \quad (\text{A8})$$

where  $E_F = \hbar \nu_0 k_F$  is the electron Fermi energy and  $k_F = \sqrt{2\pi\rho_0}$  is the Fermi wave number. As a result, this leads to

$$\mathbf{j}_0 = \frac{E_F}{2\pi\hbar} \frac{e\tau_0}{\hbar} \mathbf{F}_0 . \quad (\text{A9})$$

In the second-quantization picture, the Hamiltonian operator for  $N$  electrons in graphene in the presence of an field may be written as

$$\hat{\mathcal{H}}(t) = \sum_{j=1}^N \nu_0 \vec{\sigma} \cdot \hat{\mathbf{p}}_j - \sum_{j=1}^N e \mathbf{F}(t) \cdot \mathbf{r}_j , \quad (\text{A10})$$

where  $\vec{\sigma} = (\sigma_x, \sigma_y)$  is the Pauli-matrix vector,  $\hat{\mathbf{p}}_j = -i\hbar\nabla_j$  is the electron momentum operator, and  $\mathbf{r}_j$  is the electron position vector. For this system, we define the center-of-mass momentum operator as  $\hat{\mathbf{P}}_c = \sum_{j=1}^N \hat{\mathbf{p}}_j$ . Therefore, the Heisenberg equation gives us

$$\frac{d\hat{\mathbf{P}}_c(t)}{dt} = -\frac{\hat{\mathbf{P}}_c(t)}{\tau_0} + \frac{1}{i\hbar} [\hat{\mathbf{P}}_c(t), \hat{\mathcal{H}}(t)] = -\frac{\hat{\mathbf{P}}_c(t)}{\tau_0} + \frac{1}{i\hbar} \sum_{j=1}^N [\hat{\mathbf{p}}_j, \hat{\mathcal{H}}(t)] = -\frac{\hat{\mathbf{P}}_c(t)}{\tau_0} + e\mathbf{F}(t) , \quad (\text{A11})$$

where we have employed the momentum-relaxation time approximation. For a steady state, we have

$$\mathbf{K}_0 \equiv \frac{\mathbf{P}_0}{\hbar} = \frac{e\tau_0}{\hbar} \mathbf{F}_0 . \quad (\text{A12})$$

Finally, we are able to connect the electron surface current density with the center-of-mass wave vector in a steady state simply through

$$\mathbf{j}_0 = \frac{E_F}{2\pi\hbar} \mathbf{K}_0 . \quad (\text{A13})$$

Recalling that we have  $\mathbf{j} = \rho_0 \mathbf{v}_d$ , where  $\mathbf{v}_d$  is the drift velocity of electrons in the system, we arrive at the relation

$$\mathbf{K}_0 = \frac{2\pi\hbar\rho_0}{E_F} \mathbf{v}_d = \frac{\hbar k_F^2}{E_F} \mathbf{v}_d = \frac{k_F}{\nu_0} \mathbf{v}_d . \quad (\text{A14})$$

Consequently, for drifted electrons we find from the Lindhardt polarization function that

$$\Pi(\mathbf{q}, \omega) = 2 \int \frac{d^2\mathbf{k}}{(2\pi)^2} \{1 + \cos[\Theta_{\mathbf{k}\mathbf{q}}(\mathbf{v}_d)]\} \frac{f_0(\varepsilon_{|\mathbf{k}-\mathbf{q}|}, T) - f_0(\varepsilon_{\mathbf{k}}, T)}{\varepsilon_{|\mathbf{k}+\mathbf{K}_0|} - \varepsilon_{|\mathbf{k}-\mathbf{q}+\mathbf{K}_0|} - \hbar(\omega + i0^+)}$$

$$= 2 \int \frac{d^2 \mathbf{k}}{(2\pi)^2} \{1 + \cos[\Theta_{\mathbf{k}\mathbf{q}}(\mathbf{v}_d)]\} \frac{f_0(\varepsilon_{|\mathbf{k}-\mathbf{q}|}, T) - f_0(\varepsilon_{\mathbf{k}}, T)}{\hbar \nu_0 k_F [\mathcal{S}(\mathbf{k}, \mathbf{v}_d) - \mathcal{S}(\mathbf{k} - \mathbf{q}, \mathbf{v}_d)] - \hbar(\omega + i0^+)} , \quad (\text{A15})$$

where  $\mathbf{v}_d$  is determined by the product of the electron mobility and the external electric field  $\mathbf{F}_0$ , and

$$\mathcal{S}(\mathbf{k}, \mathbf{v}_d) = \sqrt{(k/k_F)^2 + (v_d/\nu_0)^2 + 2(\mathbf{k}/k_F) \cdot (\mathbf{v}_d/\nu_0)} , \quad (\text{A16})$$

$$\cos[\Theta_{\mathbf{k}\mathbf{q}}(\mathbf{v}_d)] = \frac{[(\mathbf{k}/k_F) + (\mathbf{v}_d/\nu_0)] \cdot [(\mathbf{k}/k_F) - (\mathbf{q}/k_F) + (\mathbf{v}_d/\nu_0)]}{\mathcal{S}(\mathbf{k}, \mathbf{v}_d) \mathcal{S}(\mathbf{k} - \mathbf{q}, \mathbf{v}_d)} . \quad (\text{A17})$$

When  $v_d/\nu_0 \ll 1$  is satisfied, we obtain

$$\mathcal{S}(\mathbf{k}, \mathbf{v}_d) \approx \frac{k}{k_F} + \left(\frac{\mathbf{k}}{k}\right) \cdot \left(\frac{\mathbf{v}_d}{\nu_0}\right) + \mathcal{O}\left[\left(\frac{v_d}{\nu_0}\right)^2\right] , \quad (\text{A18})$$

$$\mathcal{S}(\mathbf{k}, \mathbf{v}_d) - \mathcal{S}(\mathbf{k} - \mathbf{q}, \mathbf{v}_d) \approx \left(\frac{\mathbf{q}}{k}\right) \cdot \left(\frac{\mathbf{v}_d}{\nu_0}\right) + \mathcal{O}\left[\left(\frac{v_d}{\nu_0}\right)^2\right] , \quad (\text{A19})$$

and

$$\begin{aligned} \cos[\Theta_{\mathbf{k}\mathbf{q}}(\mathbf{v}_d)] &\approx \frac{[\mathbf{k} \cdot (\mathbf{k} - \mathbf{q}) + k_F(2\mathbf{k} - \mathbf{q}) \cdot (\mathbf{v}_d/\nu_0)] k|\mathbf{k} - \mathbf{q}|}{k^2|\mathbf{k} - \mathbf{q}|^2 + k_F(\mathbf{v}_d/\nu_0) \cdot [k^2(\mathbf{k} - \mathbf{q}) + \mathbf{k}|\mathbf{k} - \mathbf{q}|^2]} \approx \frac{\mathbf{k} \cdot (\mathbf{k} - \mathbf{q})}{k|\mathbf{k} - \mathbf{q}|} \\ &+ k_F \left(\frac{\mathbf{v}_d}{\nu_0}\right) \cdot \left\{ \frac{2\mathbf{k} - \mathbf{q}}{k|\mathbf{k} - \mathbf{q}|} - \left[ \frac{\mathbf{k} \cdot (\mathbf{k} - \mathbf{q})}{k|\mathbf{k} - \mathbf{q}|} \right] \left( \frac{\mathbf{k} - \mathbf{q}}{|\mathbf{k} - \mathbf{q}|^2} + \frac{\mathbf{k}}{k^2} \right) \right\} + \mathcal{O}\left[\left(\frac{v_d}{\nu_0}\right)^2\right] . \end{aligned} \quad (\text{A20})$$

---

<sup>1</sup> K. Kempa, P. Bakshi, J. Cen, and H. Xie, Phys. Rev. B **43**, 9273 (1991).

<sup>2</sup> S. Tariq, A. M. Mirza, and W. Masood, Phys. Plasmas **17**, 102705 (2010).

<sup>3</sup> M. Akbari-Moghanjoughi, Phys. Plasmas **21**, 053301 (2014).

<sup>4</sup> C.-C. Liu, W. Feng, and Y. Yao, Phys. Rev. Lett. **107**, 076802 (2011).

<sup>5</sup> E. A. Shaner, A. D. Grine, M. C. Wanke, Mark Lee, J. L. Reno, and S. J. Allen, IEEE Photon. Technol. Lett. **18**, 1925 (2006).

<sup>6</sup> V. V. Popov, T. V. Teperik, G. M. Tsymbalov, X. G. Peralta, S. J. Allen, N. J. M. Horing, and M. C. Wanke, Semicond. Sci. Technol. **19**, S71 (2004).

<sup>7</sup> A. Balassis and G. Gumbs, J. Appl. Phys. **106**, 103102 (2009).

- <sup>8</sup> A. Balassis, G. Gumbs, and D. H. Huang, Proc. SPIE **7467**, 74670O (2009).
- <sup>9</sup> S. J. Allen, D. S. Tsui, and R. A. Logan, Phys. Rev. Lett. **38**, 980 (1977).
- <sup>10</sup> D. S. Tsui, S. J. Allen, R. A. Logan, A. Kamgar, and S. N. Coopersmith, Surf. Sci. **73**, 419 (1978).
- <sup>11</sup> S. Katayama, J. Phys. Soc. Japan **60**, 1123 (1991); Surf. Sci. **263**, 359 (1992).
- <sup>12</sup> C. Steinebach, D. Heitmann, and V. Gudmundsson, Phys. Rev. B **56**, 6742 (1997).
- <sup>13</sup> B. P. van Zyl and E. Zaremba, Phys. Rev. B **59**, 2079 (1999).
- <sup>14</sup> S. A. Mikhailov, Phys. Rev. B **58**, 1517 (1998).
- <sup>15</sup> O. R. Matov, O. F. Meshkov, and, V. V. Popov, JETP **86**, 538 (1998).
- <sup>16</sup> O. R. Matov, O. V. Polischuk, and V. V. Popov, JETP **95**, 505 (2002).
- <sup>17</sup> G. Gumbs and D. H. Huang, Phys. Rev. B **75**, 115314 (2007).
- <sup>18</sup> D. H. Huang, G. Gumbs, P. M. Alsing, and D. A. Cardimona, Phys. Rev. B **77**, 165404 (2008).
- <sup>19</sup> N. J. M. Horing, E. Kamen, and H.-L. Cui, Phys. Rev. B **32**, 2184 (1985).
- <sup>20</sup> N. J. M. Horing, Phys. Rev. B **80**, 193401 (2009).
- <sup>21</sup> B. Wunsch, T. Stauber, F. Sols, and F. Guinea, New J. Phys. **8**, 318 (2006).
- <sup>22</sup> P. K. Pyatkovskiy, J. Phys.: Condens. Matt. **21**, 025506 (2009).
- <sup>23</sup> S. Das Sarma and A. Madhukar, Phys. Rev. B **23**, 805 (1981).